Author Profile

"What I first look for in a publication is to learn something I did not know.
The most important thing I learned from my parents is self-reliance. …"
This and more about Barry M. Trost can be found on page 7074.

Barry M. Trost ——— **7074 – 7076**

Obituaries

Herbert D. Kaesz (1933–2012)

Zi-Ling Xue ——— **7077 – 7078**

Books

Molecular Cluster Magnets	Richard Winpenny	*reviewed by R. Clérac* ——— **7079**
Kinetics of Chemical Reactions	Guy Marin, Gregory S. Yablonsky	*reviewed by F. J. Keil* ——— **7080**

Highlights

Geodesic Polynuclear Arene

C. Thilgen* ——— **7082 – 7084**

Synthesis of Geodesic Polynuclear Arenes and Fullerenes by Intramolecular Aryl–Aryl Coupling

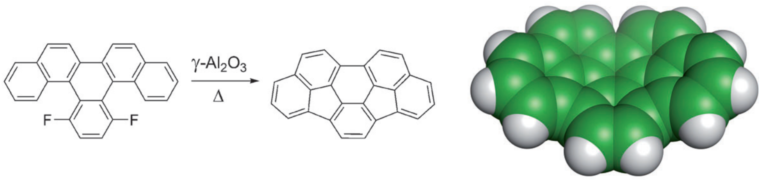

Bending over backwards to build buckybowls and -balls? For the last two decades, flash vacuum pyrolysis of chloro- and bromoarenes has been the method of choice for intramolecular aryl–aryl couplings that afford geodesic polynuclear arenes ("buckybowls") including fullerene C_{60}. Recently, even fluoroarenes were subjected under relatively mild conditions to intramolecular $C_{Ar}-C_{Ar}$ couplings by combining the cleavage of $C_{Ar}-F$ with the formation of very strong Si–F or Al–F bonds (see picture; green C, white H).

Cyclopropanes

J. Kaschel, T. F. Schneider, D. B. Werz* ——— **7085 – 7086**

One Pot, Two Phases: Iron-Catalyzed Cyclopropanation with In Situ Generated Diazomethane

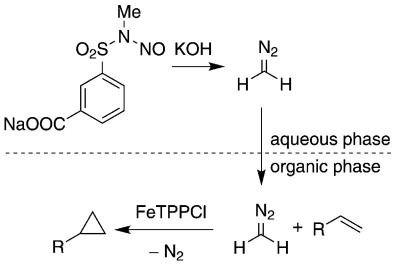

Tamed! The safe handling of diazomethane can be accomplished by a two-phase reaction. After being generated in aqueous media, the highly reactive species transfers to the organic phase and directly converts alkenes into cyclopropanes (see scheme). An air-stable iron(III) porphyrin complex serves as the catalyst.

Essays

Philosophy of Science

G. Franck* ______ **7088 – 7092**

Modern Science: A Case of Collective Intelligence? On the Role of Thought Economy and Gratifying Attention in Knowledge Production

Your attention please: Phenomenal conciousness, that is, how something feels, does not exist for an observer. As science relies on observations, it is not aware of the nature of subjectivity and thus science is not often defined as a collective intelligence. In this Essay, the roles of intelligence and attention are discussed, as well as an analysis of scientific communication and citation, in order to evaluate whether science is a case of collective intelligence.

Minireviews

Carbon Nanotubes

U. H. F. Bunz,* S. Menning,
N. Martín* ______ **7094 – 7101**

para-Connected Cyclophenylenes and Hemispherical Polyarenes: Building Blocks for Single-Walled Carbon Nanotubes?

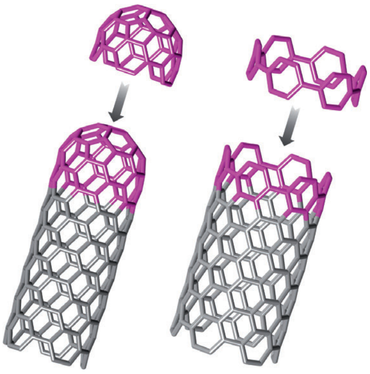

Carbon nanotubes by design? Cyclo-*para*-phenylenes are monomers for the synthesis of armchair carbon nanotubes (see picture, right), and are also attractive fluorophores that display size-dependent emission properties. Geodesic polyarenes represent a realistic alternative for the rational design of carbon nanotubes through the chemical elongation of the hydrocarbon template (left).

Smart Materials

D. J. Broer, C. M. W. Bastiaansen,
M. G. Debije,
A. P. H. J. Schenning* ______ **7102 – 7109**

Functional Organic Materials Based on Polymerized Liquid-Crystal Monomers: Supramolecular Hydrogen-Bonded Systems

Get smart: The self-assembly of liquid crystals can be used to prepare well-defined nanostructured functional materials. The picture shows a polymer film composed of hydrogen-bonded dimers and a cross-linker that curls and straightens in response to changes in the relative humidity.

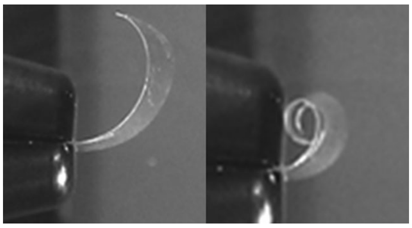

For the USA and Canada:
ANGEWANDTE CHEMIE International Edition (ISSN 1433-7851) is published weekly by Wiley-VCH, PO Box 191161, 69451 Weinheim, Germany. Air freight and mailing in the USA by Publications Expediting Inc., 200 Meacham Ave., Elmont, NY 11003. Periodicals postage paid at Jamaica, NY 11431. US POSTMASTER: send address changes to *Angewandte Chemie*, Journal Customer Services, John Wiley & Sons Inc., 350 Main St., Malden, MA 02148-5020. Annual subscription price for institutions: US$ 11.738/10.206 (valid for print and electronic / print or electronic delivery); for individuals who are personal members of a national chemical society prices are available on request. Postage and handling charges included. All prices are subject to local VAT/ sales tax.

Reviews

Biochemistry

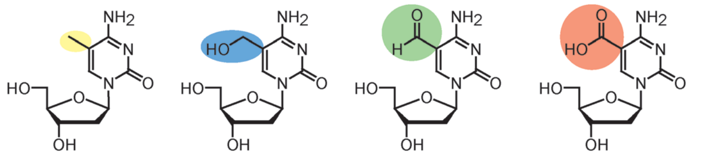

Besides their four canonical nucleobases, DNA and RNA contain a variety of highly modified nucleosides including the epigenetic bases mC, hmC, fC, and caC (see scheme), which are able to increase the chemical information content. The function of these modified bases is to generate a second level of chemical complexity in RNA and DNA in addition to the first coding level provided by the sequence of the canonical Watson–Crick bases.

Communications

Enzyme Catalysis

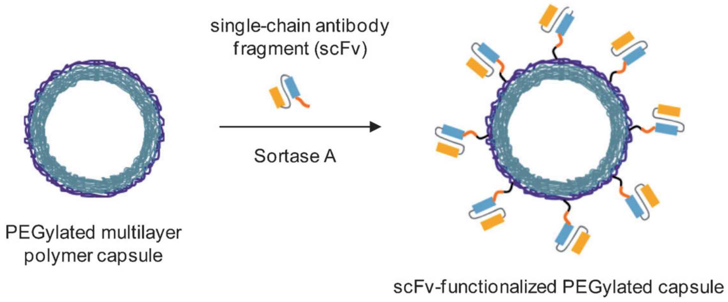

All sorted: The enzyme Sortase A was used to catalyze functionalization of PEGylated capsules with an activation-specific anti-platelet single-chain antibody (scFv). This enzymatic method allows fast, covalent, and site-directed functionalization of delivery vehicles under mild conditions. Activation-specific anti-platelet scFv-coated PEGylated capsules exhibited a high level of selective binding to thrombi, thus suggesting their potential for thrombosis therapy.

Switchable Catalyst

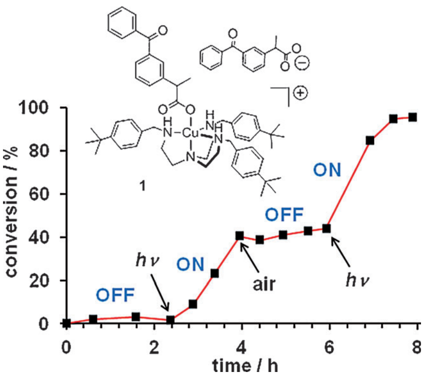

PET cat. While the copper(II) tren ketoprofenate precatalyst **1** (see picture) is inactive at room temperature in methanol, it is quantitatively and rapidly reduced to its cuprous state upon light irradiation to provide a highly reactive click catalyst. By simply introducing air into the reaction medium the catalysis can be switched off and then switched on again by bubbling argon followed by irradiation.

Nanostructures

M. Orbach, M. Lahav, P. Milko, S. G. Wolf,
M. E. van der Boom* ——— **7142 – 7145**

Setting the Environmental Conditions for Controlling Gold Nanoparticle Assemblies

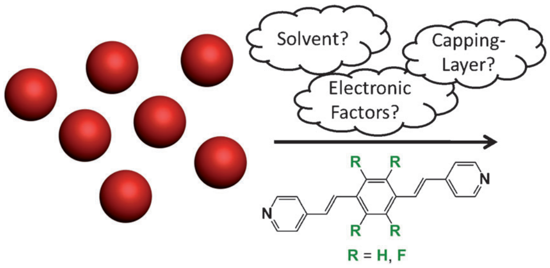

Fundamental insights into the factors that control the properties and structure of gold nanoparticle (AuNP) based assemblies enable the design and construction of new materials. The dimensions (shape and size) and the optical properties of AuNP assemblies are affected by the electronic properties of the organic cross-linker and the nature of the AuNPs.

Responsive Gels

J. Yoon, P. Bian, J. Kim, T. J. McCarthy,
R. C. Hayward* ——— **7146 – 7149**

Local Switching of Chemical Patterns through Light-Triggered Unfolding of Creased Hydrogel Surfaces

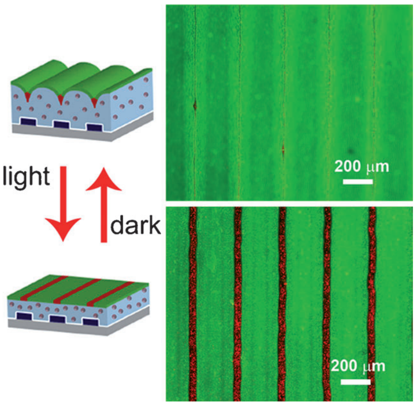

Visible light induces switching of surface chemical patterns based on hybrid gels of thermally responsive poly(*N*-isopropyl acrylamide) copolymer networks containing iron oxide nanoparticles. The swelling of these hybrid gels is reduced upon illumination (see picture), allowing controlled unfolding of creased features formed owing to an elastic surface instability.

Membrane Proteins

J. He, K. Hristova,
W. C. Wimley* ——— **7150 – 7153**

A Highly Charged Voltage-Sensor Helix Spontaneously Translocates across Membranes

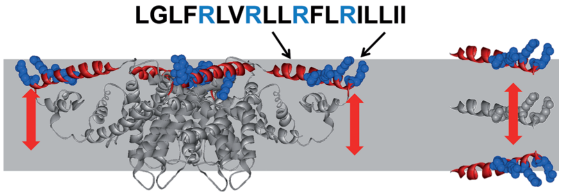

Moving freely: A recent model for voltage gating of potassium channels proposed that the four arginine residues of the voltage-sensing S4 helix (left) are in direct contact with the membrane lipids and move into the hydrocarbon core of the membrane during gating. It is demonstrated that the physical properties of the isolated S4 sequence (right) are sufficient to allow it to freely translocate across synthetic membranes.

Organic Cages

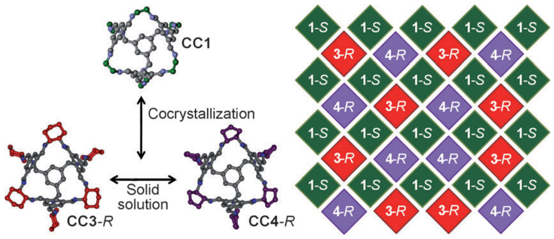

Another brick in the wall: Porous ternary cocrystals were prepared by chiral recognition between organic cage modules. One module, **CC1**, is ordered on 50% of the lattice positions with respect to two other modules, **CC3** and **CC4**, that are disordered across the other 50% of sites (see picture). There is a linear relationship between relative module composition and the cocrystal lattice parameters.

T. Hasell, S. Y. Chong, M. Schmidtmann,
D. J. Adams, A. I. Cooper* — **7154 – 7157**

Porous Organic Alloys

Silicon Chemistry

Strained but stable: An isolable silacycloprop-1-ylidene stabilized by intramolecular complexation with an iminophosphorus ylide fragment was successfully synthesized and fully characterized. The formation of this small highly strained cyclic silylene involves an unprecedented $\mathrm{Si^{IV}} \rightarrow \mathrm{Si^{II}}$ rearrangement under very mild conditions.

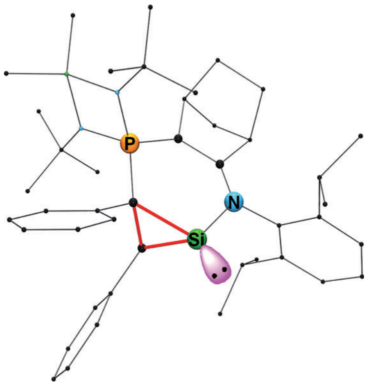

R. Rodriguez, T. Troadec, T. Kato,*
N. Saffon-Merceron, J.-M. Sotiropoulos,
A. Baceiredo* ———— **7158 – 7161**

Synthesis and Characterization of an Isolable Base-Stabilized Silacycloprop-1-ylidene

---

High-Temperature Superconductors

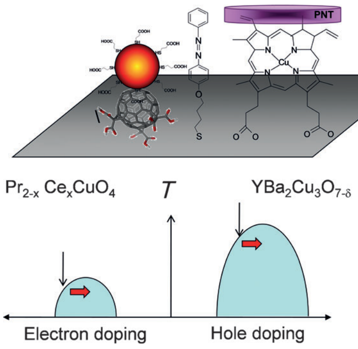

Control over the T_c value of high-T_c superconductors by self-assembled monolayers is demonstrated (T_c = critical temperature). Molecular control was achieved by adsorption of polar molecules on the superconductor surface (see scheme) that change its carrier concentration through charge transport or light-induced polarization.

I. Carmeli,* A. Lewin, E. Flekser,
I. Diamant, Q. Zhang, J. Shen, M. Gozin,
S. Richter,* Y. Dagan* —— **7162 – 7165**

Tuning the Critical Temperature of Cuprate Superconductor Films with Self-Assembled Organic Layers

---

Dynamic Membranes

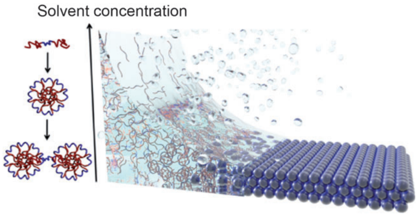

When pressure is applied to dynamic interactive membranes consisting of micelles composed of a triblock copolymer, their morphologies can be fine-tuned. Membranes with a range of porosities are accessible which can regulate and thereby control filtration performance and also display effective autonomous healing.

P. Tyagi, A. Deratani, D. Bouyer, D. Cot,
V. Gence, M. Barboiu,* T. N. T. Phan,
D. Bertin, D. Gigmes,
D. Quemener* ———— **7166 – 7170**

Dynamic Interactive Membranes with Pressure-Driven Tunable Porosity and Self-Healing Ability

Graphite Nanoneedles

R. Silva, J. Al-Sharab,
T. Asefa* ________________ **7171 – 7175**

Edge-Plane-Rich Nitrogen-Doped Carbon Nanoneedles and Efficient Metal-Free Electrocatalysts

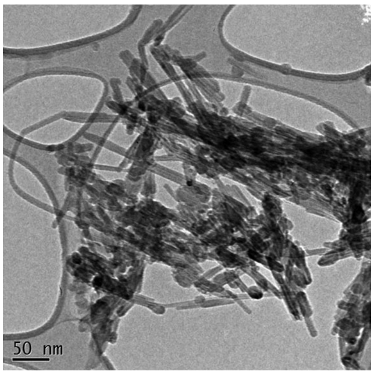

CNN news: N-doped carbon nanoneedles (CNNs) are synthesized by self-assembling core–shell nanostructures and nanoreactors around cellulose nanoneedles, and subsequent graphitization. The resulting graphitic nanoneedles (see picture) have well-organized graphitic multilayers and large proportions of N-doped edge planes. The materials serve as efficient metal-free electrocatalysts for hydrazine oxidation.

Fluorescence Imaging

S. Wang, J. Guo, T. Ono,
E. T. Kool* ______________ **7176 – 7180**

DNA Polyfluorophores for Real-Time Multicolor Tracking of Dynamic Biological Systems

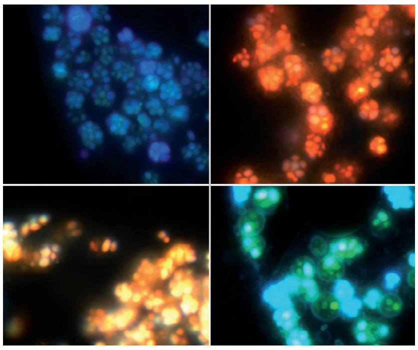

Dye-ing to live: Spectral limitations of common organic dyes make it difficult or impossible to visualize and follow multiple biological components in rapidly moving systems. The development of a multispectral set of improved DNA-scaffolded fluorophores is described. Their use in multicolor cellular imaging (see scheme) and in tracking of biological motions on the subsecond timescale is demonstrated.

Biosynthetic Engineering

J. Thirlway, R. Lewis, L. Nunns,
M. Al Nakeeb, M. Styles, A.-W. Struck,
C. P. Smith, J. Micklefield* _ **7181 – 7184**

Introduction of a Non-Natural Amino Acid into a Nonribosomal Peptide Antibiotic by Modification of Adenylation Domain Specificity

Calcium-dependent antibiotics (CDA) are cyclic lipopeptides assembled by nonribosomal peptide synthetase (NRPS) enzymes. Active site modification of the 3-methyl glutamate activating adenylation (A) domain of the CDA NRPS enables the incorporation of synthetic 3-methyl glutamine into CDA. This provides the first example of how A-domains can be engineered to introduce synthetic "non-natural" amino acids into nonribosomal peptides.

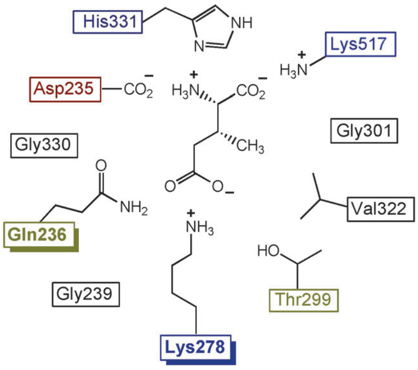

Bioimaging

A. Zhu, Q. Qu, X. Shao, B. Kong,
Y. Tian* ________________ **7185 – 7189**

Carbon-Dot-Based Dual-Emission Nanohybrid Produces a Ratiometric Fluorescent Sensor for In Vivo Imaging of Cellular Copper Ions

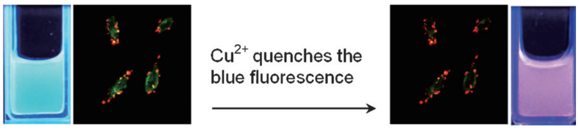

A sensitive biosensor: A strategy for the intracellular imaging of Cu^{2+} ions has been developed by integrating a recognition molecule, *N*-(2-aminoethyl)-*N*,*N*,*N*′-tris(pyridin-2-ylmethyl)ethane-1,2-diamine (AE-TPEA), into a hybrid system composed of carbon and CdSe/ZnS quantum dots.

Fischer–Tropsch Synthesis

A. C. J. Koeken,* H. M. Torres Galvis,
T. Davidian, M. Ruitenbeek,
K. P. de Jong* ——— 7190–7193

Suppression of Carbon Deposition in the Iron-Catalyzed Production of Lower Olefins from Synthesis Gas

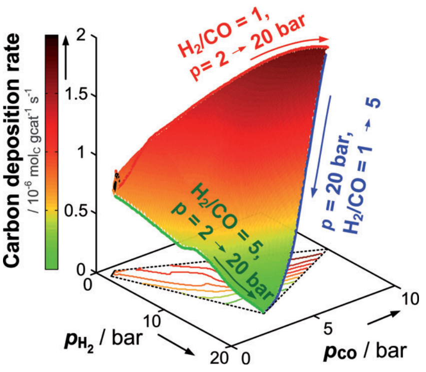

Pressure leverage: A tapered-element oscillating microbalance was used to evaluate carbon deposition on a highly selective and active supported iron catalyst for the production of lower olefins. With increasing pressure, the H_2/CO ratio had a profound effect on the carbon deposition rate and accordingly, conditions leading to minimal carbon deposition, low methane selectivity, and high olefin selectivity were identified.

Polyoxometalates

M. Sanchez Sanchez, F. Girgsdies,
M. Jastak, P. Kube, R. Schlögl,
A. Trunschke* ——— 7194–7197

Aiding the Self-Assembly of Supramolecular Polyoxometalates under Hydrothermal Conditions To Give Precursors of Complex Functional Oxides

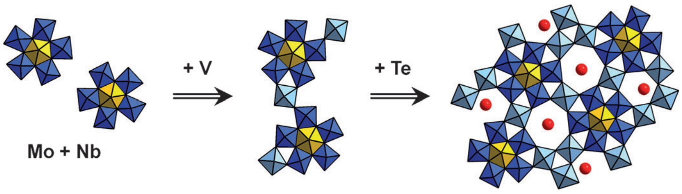

In situ Raman spectroscopy allows insight into molecular processes under hydrothermal conditions during synthesis of complex nanostructured MoVTeNb oxides (see picture: Nb yellow, Mo blue, V/Mo pale blue, Te red). Based on the knowledge acquired, the synthesis can be more efficiently directed towards the desired product with improved functionality.

DNA Recognition and Scission

T. Ishizuka, J. Yang, M. Komiyama,*
Y. Xu* ——— 7198–7202

G-Rich Sequence-Specific Recognition and Scission of Human Genome by PNA/DNA Hybrid G-Quadruplex Formation

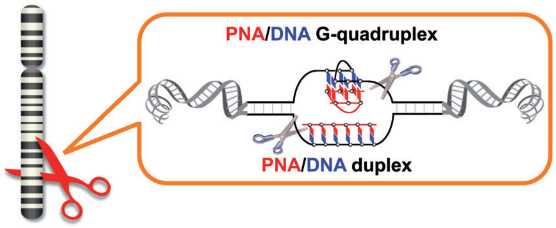

Hole in one: A single peptide nucleic acid (PNA) effectively targets the G-rich region in double-stranded DNA through formation of a PNA/DNA hybrid G-quadruplex. Only one target site in the whole human genome was selectively cleaved by the hybrid G-quadruplex. Such site-selective scission of DNA is central to gene manipulation for molecular biology, biotechnology, and therapy.

siRNA Delivery

S. J. Lee, M. S. Huh, S. Y. Lee, S. Min,
S. Lee, H. Koo, J.-U. Chu, K. E. Lee,
H. Jeon, Y. Choi, K. Choi, Y. Byun,
S. Y. Jeong, K. Park, K. Kim,*
I. C. Kwon* ——— 7203–7207

Tumor-Homing Poly-siRNA/Glycol Chitosan Self-Cross-Linked Nanoparticles for Systemic siRNA Delivery in Cancer Treatment

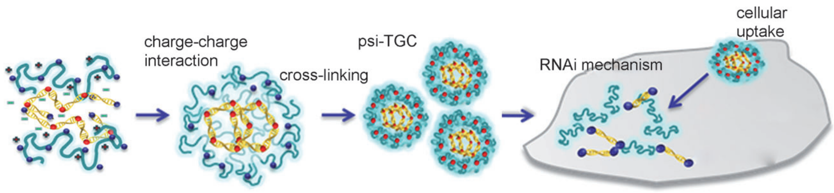

The condensed version: Thiolated glycol chitosan can form stable nanoparticles with polymerized siRNAs through charge–charge interactions and self-cross-linking (see scheme). This poly-siRNA/glycol chitosan nanoparticles (psi-TGC) provided sufficient in vivo stability for systemic delivery of siRNAs. Knockdown of tumor proteins by psi-TGC resulted in a reduction in tumor size and vascularization.

Supramolecular Chemistry

O. Kotova, R. Daly, C. M. G. dos Santos,
M. Boese, P. E. Kruger, J. J. Boland,*
T. Gunnlaugsson* ________ 7208 – 7212

Europium-Directed Self-Assembly of a Luminescent Supramolecular Gel from a Tripodal Terpyridine-Based Ligand

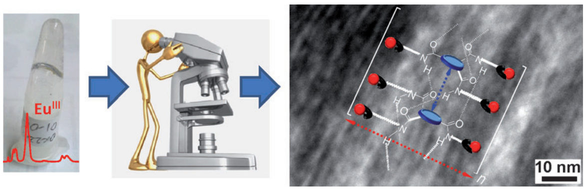

Eu^{III}, the last piece in the puzzle: Europium-induced self-assembly of ligands having a C_3-symmetrical benzene-1,3,5-tricarboxamide core results in the formation of luminescent gels. Supramolecular polymers are formed through hydrogen bonding between the ligands. The polymers are then brought together into the gel assembly through the coordination of terpyridine ends by Eu^{III} ions (blue dashed arrow: distance between two ligands in the strand direction).

Pt Electrocatalysts

B. Y. Xia, W. T. Ng, H. B. Wu, X. Wang,*
X. W. Lou* ________ 7213 – 7216

Self-Supported Interconnected Pt Nanoassemblies as Highly Stable Electrocatalysts for Low-Temperature Fuel Cells

In it for the long haul: Clusters of Pt nanowires (3D Pt nanoassemblies, Pt NA) serve as an electrocatalyst for low-temperature fuel cells. These Pt nanoassemblies exhibit remarkably high stability following thousands of voltage cycles (see graph) and good catalytic activity, when compared with a commercial Pt catalyst and 20% wt Pt catalyst supported on carbon black (20% Pt/CB).

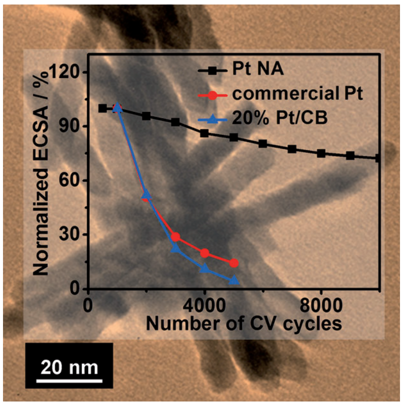

Metallopeptides

R. Kundu, P. R. Cushing, B. V. Popp,
Y. Zhao, D. R. Madden,*
Z. T. Ball* ________ 7217 – 7220

Hybrid Organic–Inorganic Inhibitors of a PDZ Interaction that Regulates the Endocytic Fate of CFTR

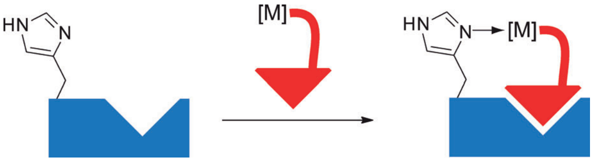

Together strong: Cooperative binding of organic (see picture, red) and inorganic fragments provides a strategy for the potent inhibition of protein–protein interactions. By targeting specific Lewis basic side chains in peripheral regions of the binding site for coordination to a rhodium(II) center, the affinity of otherwise weak ligands is improved.

Topological Insulators

L. Müchler, H. J. Zhang, S. Chadov,
B. H. Yan, F. Casper, J. Kübler, S. C. Zhang,
C. Felser* ________ 7221 – 7225

Topological Insulators from a Chemist's Perspective

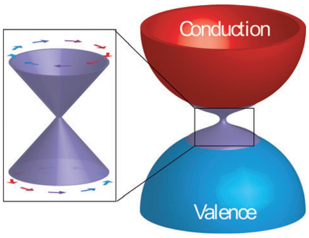

Heavy stuff: Topological insulators are formed of heavy atoms and host special surface or edge states. The electronic structure is characterized by a Dirac cone within a bulk band gap (see picture) that is generated by strong spin–orbit coupling. A chemist's perspective in terms of bonds, bands, symmetry, and nuclear charge is provided.

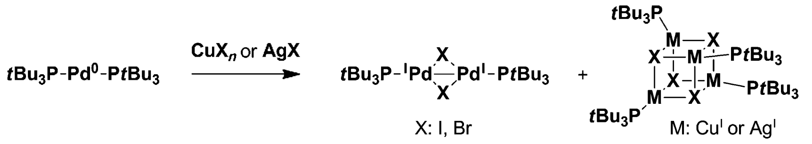

Challenging a catalytic cycle: Pd^0 catalysts are readily oxidized by Cu and Ag salts to give dinuclear Pd$^{\rm I}$ complexes and Cu$^{\rm I}$ or Ag$^{\rm I}$ cubanes (see scheme). The reactivities of the resulting Pd$^{\rm I}$ dimers are consistent with several observations of additive effects in cross-coupling chemistry. The results indicate the possibility for alternative catalytic cycles involving dinuclear Pd$^{\rm I}$ complexes over the currently accepted synergistic cycles involving Pd^0/Pd$^{\rm II}$ intermediates and Cu or Ag.

Catalysis

M. Aufiero, F. Proutiere,
F. Schoenebeck* ———— **7226 – 7230**

Redox Reactions in Palladium Catalysis: On the Accelerating and/or Inhibiting Effects of Copper and Silver Salt Additives in Cross-Coupling Chemistry Involving Electron-rich Phosphine Ligands

It's just an illusion: Above a critical chain length, where oligomers contain five or more recognition units, apparently infinite donor–acceptor polypseudorotaxanes are formed in the solid state (see picture). X-ray crystallographic analyses of three different examples have shown that although the oligomeric chains are undoubtedly discrete and monodisperse, they nevertheless appear to be infinite in the crystal.

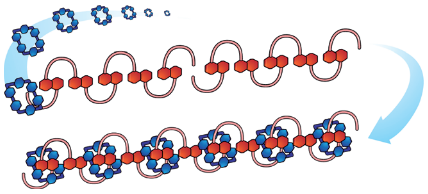

Supramolecular Crystal Engineering

Z. Zhu, H. Li, Z. Liu, J. Lei, H. Zhang,
Y. Y. Botros, C. L. Stern, A. A. Sarjeant,*
J. F. Stoddart,*
H. M. Colquhoun* ———— **7231 – 7235**

Oligomeric Pseudorotaxanes Adopting Infinite-Chain Lattice Superstructures

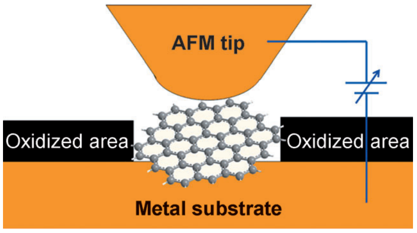

Cut into pieces: The π-electron distribution in nanographene fragments isolated between oxidized graphene areas is investigated using scanning probe microscopy (see picture). The edge-shape-dependent localization and migration of the Clar sextet explains the observed π-state distributions and enables investigation of the electronic properties.

Electronic Structure

S. Fujii,* T. Enoki* ———— **7236 – 7241**

Clar's Aromatic Sextet and π-Electron Distribution in Nanographene

Diverse opportunities: A Rhodium(III)-catalyzed *ortho*-selective olefination of arenes using a novel triazene as a directing group is reported. This method exhibits substantial post-functionalization synthetic versatility, overcoming a vital limitation in C$_{sp^2}$–H activation/functionalization products: restricted structural diversity.

Functionalizable Directing Groups

C. Wang, H. Chen, Z. Wang, J. Chen,
Y. Huang* ———— **7242 – 7245**

Rhodium(III)-Catalyzed C–H Activation of Arenes Using a Versatile and Removable Triazene Directing Group

Back Cover

Post-Translational Modifications

A novel post-translationally modified amino acid, crotonyllysine (Kcr), was genetically incorporated into proteins in bacterial and mammalian cells using an evolved pyrrolysyl-tRNA/synthetase-tRNA pair. The ability to produce histones with homogenous, site-specific Kcr modifications will be valuable in elucidating the biological role of this recently identified post-translational modification.

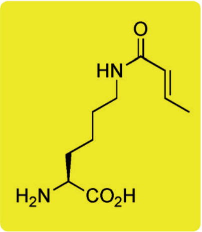

Oxidative Amidation

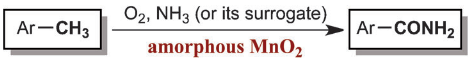

$$\mathrm{Ar{-}CH_3} \xrightarrow[\text{amorphous MnO}_2]{\mathrm{O_2},\ \mathrm{NH_3}\text{ (or its surrogate)}} \mathrm{Ar{-}CONH_2}$$

In the presence of amorphous MnO_2, various methylarenes (even with two or more methyl groups) could be selectively converted into the corresponding primary monoamides in moderate to high yields. The observed catalysis was truly heterogeneous, and the retrieved amorphous MnO_2 catalyst could be reused without an appreciable loss of its catalytic performance.

Drug Delivery

Polymerizable and hydrolytically cleavable dexamethasone (DEX, red dot in picture) derivatives were covalently entrapped in core-cross-linked polymeric micelles that were prepared from a thermosensitive block copolymer (yellow and gray building block). By varying the oxidation degree of the thioether in the drug linker, the release rate of DEX could be controlled. The DEX-loaded micelles were used for efficient treatment of inflammatory arthritis in two animal models.

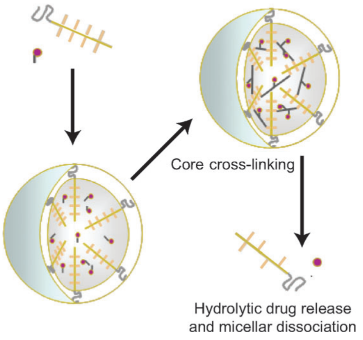

Radical-Cation Reactions

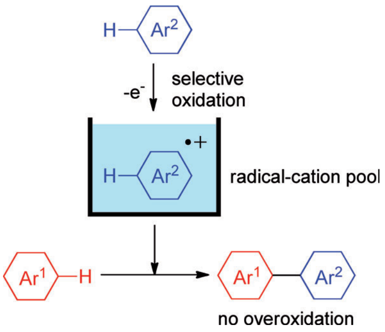

Pool and couple: A method for oxidative C–H/C–H cross-coupling has been developed using "radical-cation pools". Aromatic compounds react with aryl radical cations, which are generated and accumulated by low-temperature electrolysis (see scheme). This method avoids both the nonselective oxidation of substrates and oxidation of products and effects the C–H/C–H cross-coupling of aromatic compounds without metal complexes and chemical oxidants.

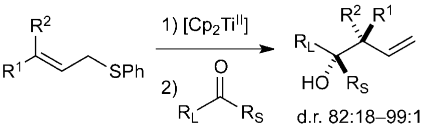

Unsymmetrical ketones and allyltitanocenes generated by the desulfurizative titanation of γ,γ-disubstituted allyl phenyl sulfides react under highly diastereoselective construction of adjacent quaternary stereocenters (see scheme; $R_L =$ large group, $R_S =$ small group). The title reaction is stereospecific: the *anti-* and *syn*-homoallylic alcohols are obtained by the reaction of *E-* and *Z*-allylic sulfides, respectively.

Synthetic Methods

T. Takeda,* M. Yamamoto, S. Yoshida, A. Tsubouchi ______ **7263–7266**

Highly Diastereoselective Construction of Acyclic Systems with Two Adjacent Quaternary Stereocenters by Allylation of Ketones

---

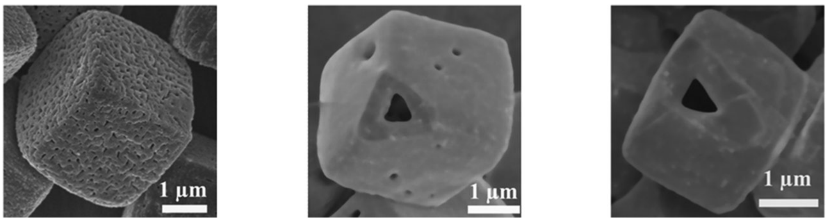

Kept cubic: MnS microboxes, which act as an anode material for lithium ion batteries, are synthesized by a simple H_2S gas sulfidation approach (TEM images show porous and hollow microcubes and a microbox). The formation of the single crystals is aided by the intrinsic cubic crystal structure and the nearly cubic shape of the $MnCO_3$ precursor.

Hollow Structures

L. Zhang, L. Zhou, H. B. Wu, R. Xu, X. W. (David) Lou* ______ **7267–7270**

Unusual Formation of Single-Crystal Manganese Sulfide Microboxes Co-mediated by the Cubic Crystal Structure and Shape

---

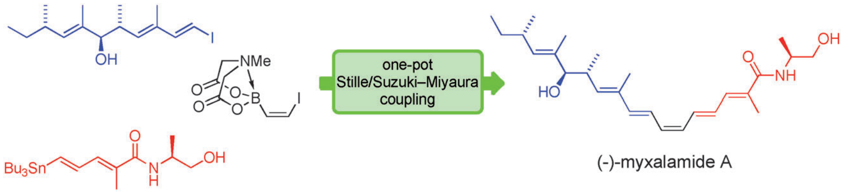

The MIDA touch: A concise and highly convergent protecting-group-free total synthesis of (−)-myxalamide A involves a stereoselective vinylogous Mukaiyama aldol reaction of a vinylketene silyl N,O-acetal, together with a one-pot Stille/Suzuki–Miyaura cross-coupling reaction using Burke's *N*-methyliminodiacetic acid (MIDA) boronate to connect left- and right-hand fragments of the molecule (see scheme).

Natural Product Synthesis

K. Fujita, R. Matsui, T. Suzuki, S. Kobayashi* ______ **7271–7274**

Concise Total Synthesis of (−)-Myxalamide A

Peroxide in, phenol out: The catalyst $[\gamma\text{-PW}_{10}O_{38}V_2(\mu\text{-OH})_2]^{3-}$ showed high activity in the hydroxylation of various aromatic compounds with aqueous H_2O_2. The system was regioselective, producing *para*-phenols from monosubstituted benzene derivatives. Furthermore, alkylarenes with reactive side-chain C_{sp^3}–H bonds could be chemoselectively hydroxylated without significant formation of side-chain oxygenated products.

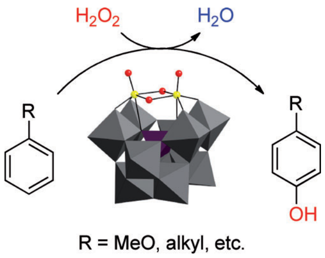

Polyoxometalate Catalysis

K. Kamata, T. Yamaura, N. Mizuno* ______ **7275–7278**

Chemo- and Regioselective Direct Hydroxylation of Arenes with Hydrogen Peroxide Catalyzed by a Divanadium-Substituted Phosphotungstate

Organocatalysis

T. Hashimoto, H. Kimura, Y. Kawamata, K. Maruoka* ______ 7279 – 7281

A Catalytic Asymmetric Ugi-type Reaction With Acyclic Azomethine Imines

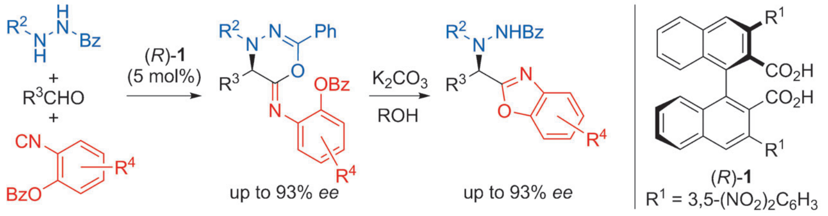

An unconventional Ugi: A catalytic asymmetric Ugi-type reaction can be realized by use of *N*′-alkylbenzohydrazide, instead of a conventional amine, in the presence of an axially chiral dicarboxylic acid. The reaction proceeds through a key acyclic azomethine imine intermediate, which has recently emerged as a promising electrophile in asymmetric catalysis.

Cascade Reactions

X.-S. Zhang, X.-X. Song, H. Li, S.-L. Zhang, X. Chen, X.-H. Yu,* W. Wang* ______ 7282 – 7286

An Organocatalytic Cascade Approach toward Polysubstituted Quinolines and Chiral 1,4-Dihydroquinolines–Unanticipated Effect of N-Protecting Groups

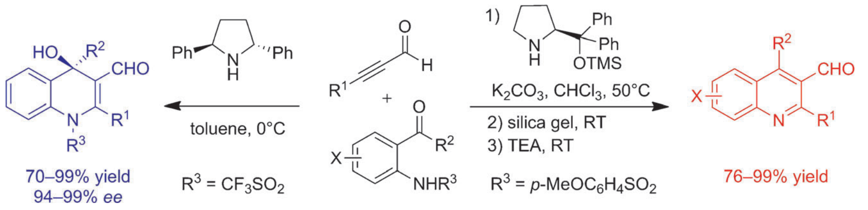

A matter of protection: The outcome of a divergent organocatalytic aza-Michael/aldol cascade process toward quinolines and 1,4-dihydroquinolines depends on the choice of the N-protecting group (see scheme; TEA = triethylamine, TMS = trimethylsilyl). Use of an electron-donating sulfonyl group results in an unanticipated aza-Michael/aldol/aromatization cascade to give polysubstituted quinolines (right). In contrast, chiral 1,4-dihydroquinolines are obtained with an electron-withdrawing sulfonyl group (left).

Micelle Formation

U. Y. Lee, N. M. Oh, D. S. Kwag, K. T. Oh, Y. T. Oh, Y. S. Youn, E. S. Lee* ______ 7287 – 7291

Facile Synthesis of Multimeric Micelles

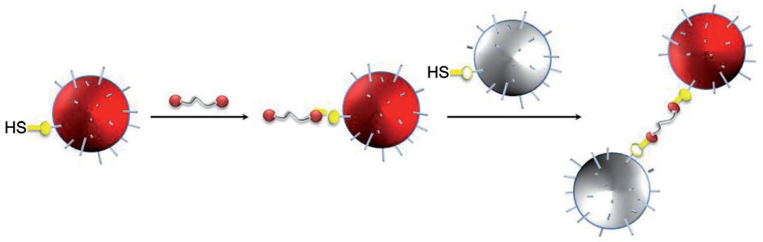

Bringing it all together: Synthesis of a dimeric micelle (see scheme) is shown to produce specifically linked Janus-like micelles. The reaction conditions for dimeric micelle formation were optimized and the resulting micelles characterized. Trimeric, tetrameric, and multimeric micelles were also synthesized using the same technique.

Quinolines

X. Ji, H. Huang, Y. Li, H. Chen, H. Jiang* ______ 7292 – 7296

Palladium-Catalyzed Sequential Formation of C–C Bonds: Efficient Assembly of 2-Substituted and 2,3-Disubstituted Quinolines

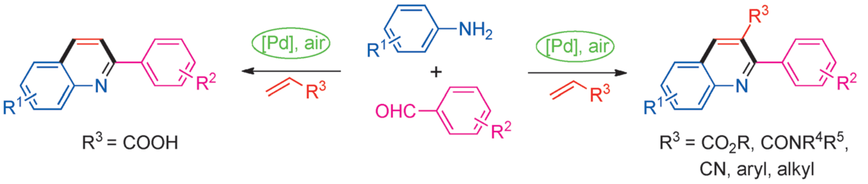

A series of substituted quinolines was prepared from arylamines, aldehydes, and terminal olefins (see scheme). The palladium-catalyzed sequential formation of C–C bonds proceeds smoothly with both electron-deficient and electron-rich olefins. When acrylic acid is used as terminal olefin, decarboxylation occurs to provide 2-substituted quinolines.

Laser Spectroscopy

C. M. Choi, D. H. Choi, J. Heo, N. J. Kim,* S. K. Kim* ———— **7297 – 7300**

Ultraviolet–Ultraviolet Hole Burning Spectroscopy in a Quadrupole Ion Trap: Dibenzo[18]crown-6 Complexes with Alkali Metal Cations

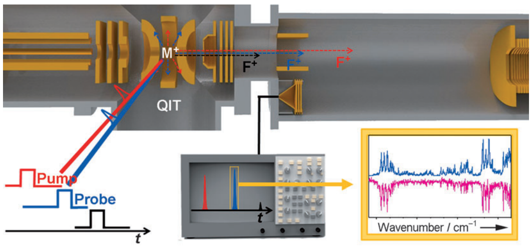

Conformation selective: A new technique of ultraviolet–ultraviolet hole burning spectroscopy that can be applied to ions stored in a quadrupole ion trap (QIT) is developed and used to obtain the conformation-selective electronic spectra of dibenzo[18]crown-6 complexes with alkali metal cations (M^+, see picture; F^+ = fragment).

N-Heterocycles

L. Liu, L. Zhang* ———— **7301 – 7304**

Access to Electron-Rich Arene-Fused Hexahydroquinolizinones through a Gold-Catalysis-Initiated Cascade Process

Golden Cascade: With a tethered, electron-rich arene as the internal nucleophile, a gold-catalyzed amide cyclization to an alkyne initiates a cascade process that ends with a Ferrier rearrangement. Electron-rich arene-bearing hexahydroquinolizin-2-ones are formed in good yields and can be converted into indole alkaloids in only a few steps.

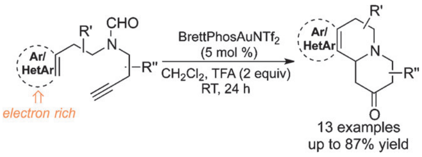

Homogeneous Catalysis

Y. Oonishi,* Y. Kitano, Y. Sato* ———— **7305 – 7308**

C_{sp^3}–H Bond Activation Triggered by Formation of Metallacycles: Rhodium(I)-Catalyzed Cyclopropanation/Cyclization of Allenynes

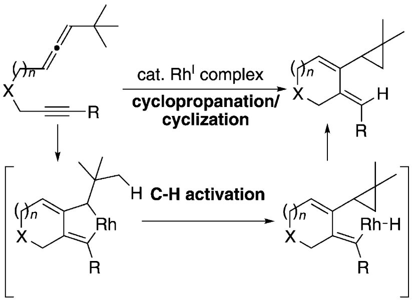

Giving direction: An C_{sp^3}–H bond activation directed by a rhodacycle intermediate has been found to occur in a Rh^I-catalyzed reaction between an allene moiety having a *tert*-butyl substituent, and tethered alkynes. Cyclic compounds containing a cyclopropane ring were obtained in good to high yields (up to 92%).

Inside Cover

Asymmetric Catalysis

D. T. Cohen, C. C. Eichman, E. M. Phillips, E. R. Zarefsky, K. A. Scheidt* ———— **7309 – 7313**

Catalytic Dynamic Kinetic Resolutions with N-Heterocyclic Carbenes: Asymmetric Synthesis of Highly Substituted β-Lactones

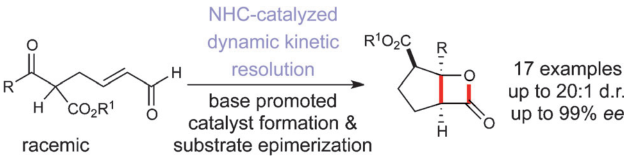

New DKR type: An N-heterocyclic carbene (NHC)-catalyzed dynamic kinetic resolution of racemic α-substituted β-keto esters has been developed. This method relies on the epimerization of an NHC-enol intermediate before subsequent aldol/acylation events. Highly substituted β-lactones are produced in good yield with good to excellent selectivities (see scheme).

Asymmetric Catalysis

D. Audisio, M. Luparia, M. T. Oliveira, D. Klütt, N. Maulide* ______ 7314–7317

Diastereodivergent De-epimerization in Catalytic Asymmetric Allylic Alkylation

Diastereomers made to order: In an unprecedented ligand-controlled process a racemic mixture of four stereoisomers can be converted with high selectivity into each one of the diastereomers of the product, at will (see scheme). The mechanism of this deracemization of epimers, that is, a de-epimerization, was also studied.

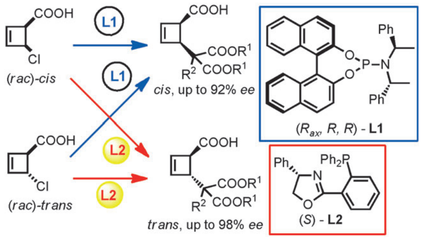

C–H Activation

H. Wang, F. Glorius* ______ 7318–7322

Mild Rhodium(III)-Catalyzed C–H Activation and Intermolecular Annulation with Allenes

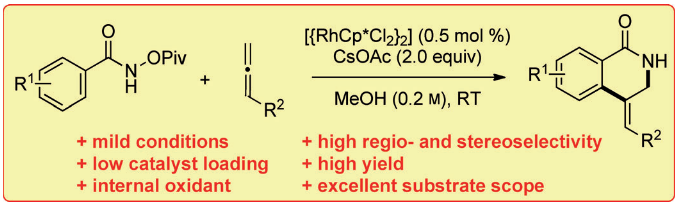

All(enes) great! A novel Rh^{III}-catalyzed oxidative coupling with allenes under mild conditions provides heterocycles with exocyclic double bonds. This reaction features low catalyst loadings, high regio- and stereoselectivity, and excellent substrate scope. The products were derivatized and preliminary mechanistic studies were conducted.

Catalyzed CO_2 Reduction

M. Khandelwal, R. J. Wehmschulte* ______ 7323–7326

Deoxygenative Reduction of Carbon Dioxide to Methane, Toluene, and Diphenylmethane with $[Et_2Al]^+$ as Catalyst

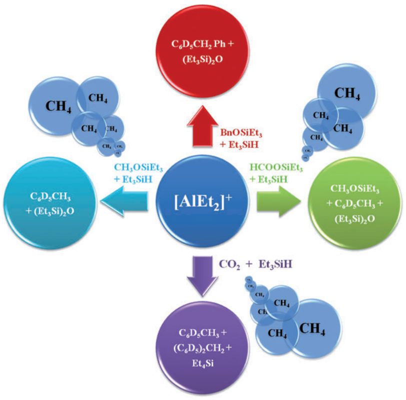

The strong Lewis acid $[Et_2Al]^+$ catalyzes the reduction of carbon dioxide with hydrosilanes under mild conditions to methane. In benzene solution, the side products toluene and diphenylmethane are also obtained through Lewis acid catalyzed benzene alkylation by reaction intermediates.

VIP

Glycomimetics

F. P. C. Binder, K. Lemme, R. C. Preston, B. Ernst* ______ 7327–7331

Sialyl Lewis^x: A "Pre-Organized Water Oligomer"?

Front Cover

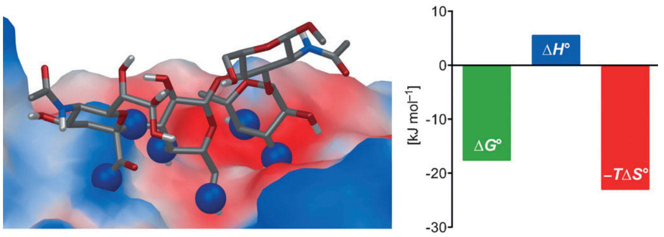

Organized and released: Sialyl Lewis^x (sLe^x) represents a "pre-organized water oligomer", that is, a surrogate for clustered water molecules attached to a scaffold. The impetus for sLe^x binding to E-selectin is shown to be the high degree of pre-organization allowing an array of directed hydrogen bonds, and the entropic benefit of the release of water molecules from the large binding interface to bulk water (see picture).

Service

Angewandte Corrigendum

The authors of this Communication have noticed that in the top panel of Figure 1 B the *x* axis on the plot (and inset) is erroneously offset by 80 nm: the *x* axis range of the main plot should be from 420 nm to 670 nm, instead of 500 nm to 750 nm. The plot (and inset) with the corrected *x* axis is shown below. All other results and conclusions of the paper remain unaffected.

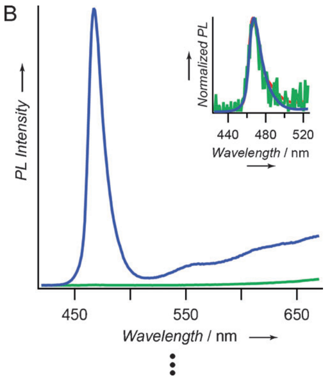

Figure 1. [...] B) Photoluminescence spectra of CdS nanorods (top), [...] obtained from hot injection (red), cation exchange (green), and post-exchange purification (blue). [...] Inset of B: Normalized photoluminescence showing similarity in the photoluminescence peak positions between samples obtained from the three different methods. [...]

Highly Luminescent Nanocrystals From Removal of Impurity Atoms Residual From Ion-Exchange Synthesis

P. K. Jain, B. J. Beberwyck,
L.-K. Fong, M. J. Polking,
A. P. Alivisatos* ______ **2387–2390**

Angew. Chem. Int. Ed. **2012**, *51*

DOI: 10.1002/anie.201107452